◆ Human Brain Mapping 38:2424–2440 (2017) ◆

Sensory Tractography and Robot-Quantified Proprioception in Hemiparetic Children with Perinatal Stroke

Andrea M. Kuczynski,[1,2] Helen L. Carlson,[2] Catherine Lebel,[1,3] Jacquie A. Hodge,[2] Sean P. Dukelow,[1,4] Jennifer A. Semrau,[1,4] and Adam Kirton[1,2,4]*

[1]*University of Calgary, Calgary, Alberta, Canada*
[2]*Section of Neurology, Department of Pediatrics, Alberta Children's Hospital, Calgary, Alberta, Canada*
[3]*Department of Radiology, Alberta Children's Hospital, Calgary, Alberta, Canada*
[4]*Department of Clinical Neurosciences, Hotchkiss Brain Institute, Calgary, Alberta, Canada*

Abstract: Perinatal stroke causes most hemiparetic cerebral palsy, resulting in lifelong disability. We have demonstrated the ability of robots to quantify sensory dysfunction in hemiparetic children but the relationship between such deficits and sensory tract structural connectivity has not been explored. It was aimed to characterize the relationship between the dorsal column medial lemniscus (DCML) pathway connectivity and proprioceptive dysfunction in children with perinatal stroke. Twenty-nine participants (6–19 years old) with MRI-classified, unilateral perinatal ischemic stroke (14 arterial, 15 venous), and upper extremity deficits were recruited from a population-based cohort and compared with 21 healthy controls. Diffusion tensor imaging (DTI) defined DCML tracts and five diffusion properties were quantified: fractional anisotropy (FA), mean, radial, and axial diffusivities (MD, RD, AD), and fiber count. A robotic exoskeleton (KINARM) tested upper limb proprioception in an augmented reality environment. Correlations between robotic measures and sensory tract diffusion parameters were evaluated. Lesioned hemisphere sensory tracts demonstrated lower FA and higher MD, RD, and AD compared with the non-dominant hemisphere of controls. Dominant (contralesional) hemisphere tracts were not different from controls. Both arterial and venous stroke groups demonstrated impairments in proprioception that correlated with lesioned hemisphere DCML tract diffusion properties. Sensory tract connectivity is altered in the lesioned hemisphere of hemiparetic children with perinatal stroke. A correlation between lesioned DCML tract diffusion properties and robotic proprioceptive measures suggests clinical relevance and a possible target for therapeutic intervention. *Hum Brain Mapp 38:2424–2440, 2017.*

Key words: perinatal stroke; sensory; tractography; position sense; kinesthesia; proprioception; robotics

Contract grant sponsors: Alberta Children's Hospital CIHR Trainee Studentship, Alberta Innovates – Health Solutions graduate studentship, Hotchkiss Brain Institute's Robertson Fund, and a Cerebral Palsy International Research Foundation Grant

Conflicts of Interest: CL's spouse is an employee of General Electric. All other authors confirm no conflicts of interest.

*Correspondence to: Dr. Adam Kirton Section of Neurology, Alberta Children's Hospital 2888 Shaganappi Trail NW, Calgary, AB, Canada T3B 6A8. E-mail: adam.kirton@albertahealthservices.ca

Received for publication 12 October 2016; Revised 27 December 2016; Accepted 16 January 2017.

DOI: 10.1002/hbm.23530
Published online 8 February 2017 in Wiley Online Library (wileyonlinelibrary.com).

INTRODUCTION

Perinatal ischemic stroke is a common focal brain injury occurring between gestational week 20 and the 28th postnatal day [Raju et al., 2007]. Neuroimaging studies have defined two common ischemic stroke diseases: arterial ischemic stroke (AIS) and periventricular venous infarction (PVI) [Kirton et al., 2008]. Most AIS result from middle cerebral artery (MCA) occlusion in term newborns, resulting in damage to cortical and subcortical structures [Kirton et al., 2011]. In contrast, PVI is a subcortical white matter lesion occurring preterm, *in utero* secondary to germinal matrix hemorrhage. Both AIS and PVI typically injure brain structures involved in motor control, resulting in contralateral motor dysfunction (hemiparetic cerebral palsy, CP) [Kirton and DeVeber, 2013]. In addition to motor disability, sensory impairments may also be common in CP, including deficits in passive motion sense [Tizard et al., 1954; Van Heest et al., 1993; Wann, 1991], tactile discrimination [Auld et al., 2012], and stereognosis [Tizard et al., 1954; Van Heest et al., 1993]. However, previous studies have not been specific to perinatal ischemic stroke and tools for the objective quantification of sensory function have been limited.

Proprioception is a complex somatosensory modality that utilizes input from muscle, joint, and cutaneous afferent fibers to perceive position (position sense) and motion (kinesthesia) generated by the body [Proske and Gandevia, 2012; Sherrington, 1907]. Intact proprioception is essential for optimal motor control [Scott, 2012], maintaining the cortical representation of the body [Schabrun and Hillier, 2009], and is likely necessary for recovery of movement and function after brain injury [Tyson et al., 2008]. The dorsal column medial lemniscus (DCML) pathway primarily carries proprioceptive information from peripheral receptors to the somatosensory cortex in the post-central gyrus. This information is further processed in the posterior parietal cortex, as well as Brodmann's area 7 for visual-proprioceptive integration [Andersen, 1997; Lacquaniti et al., 1995]. Studies in adult stroke survivors have found proprioceptive deficits to be associated with damage to parietal and temporal lobe regions [Findlater et al., 2016; Kenzie et al., 2015].

Historically, a major challenge in quantifying proprioception has been that existing clinical tools lack sensitivity to small changes, offer poor reliability, and carry the potential for examiner bias [Elangovan et al., 2014; Garraway et al., 1976; Lincoln, 1991]. Advances in robotic technology provide more detailed, objective, and reliable methods for studying proprioceptive function in healthy and diseased populations. The kinesiological instrument for normal and altered reaching movements (KINARM) exoskeleton robot has been developed to objectively assess position sense [Dukelow et al., 2010], kinesthesia [Semrau et al., 2013, 2015], and unilateral motor function [Coderre et al., 2010] in healthy individuals and adult stroke survivors. We recently used KINARM to characterize position sense [Kuczynski et al., 2016] and kinesthetic [Kuczynski et al., 2016, under review] deficits in children with perinatal stroke. Dysfunction in proprioception was common, associated with stroke type, and correlated with functional disability, supporting clinical relevance of proprioceptive dysfunction in daily function. However, the neuroanatomical alterations and physiological mechanisms that underlie such proprioceptive dysfunction after perinatal stroke are unknown.

Diffusion tensor imaging (DTI) can evaluate structural connectivity by examining the direction and intensity of water diffusion in white matter tracts to reveal the characteristics of tissue microstructure, facilitating the study of sensory pathways [Lai et al., 2014]. Multiple DTI studies evaluating the corticospinal tract after perinatal stroke [van der Aa et al., 2013; Jaspers et al., 2015; Lennartsson et al., 2015; Roze et al., 2012] have defined imaging biomarkers associated with clinical outcome such as decreased fractional anisotropy (FA) in the lesioned hemisphere. Whether diffusion imaging of sensory pathway structural connectivity carries the same potential has not been determined.

In this prospective case-control study, we compared DCML diffusion parameters in hemiparetic children with perinatal stroke and typically developing controls. We hypothesized that sensory tract diffusion properties in the lesioned hemisphere would differ between stroke groups and controls, the degree of which would correlate with robot-quantified position sense and kinesthetic impairments.

METHODS

Participants

Participants were enrolled through the Alberta Perinatal Stroke Project, a population-based research cohort. Inclusion criteria were age 6–19 years, term birth ($\geq$36 weeks), unilateral MRI-confirmed perinatal stroke (arterial or venous) [Kirton et al., 2008], clinical confirmation of symptomatic hemiparetic CP including Pediatric Stroke Outcome Measure (PSOM) [Kitchen et al., 2012] sensorimotor component $\geq$0.5, Manual Abilities Classification System (MACS) [Eliasson et al., 2006] grade I–IV, and child and parent perceived functional limitations. Exclusion criteria were: (1) multifocal stroke, (2) other neurological disorders not attributable to stroke, (3) severe hemiparesis (MACS grade V), (4) severe spasticity (Modified Ashworth Scale = 4) or contracture, (5) upper limb surgery or botulinum toxin injections in the last 6 months, and (6) inability to comply with testing protocols.

Typically developing children comparable in age and sex were recruited from the community and underwent identical evaluations. Healthy controls were right-handed per the Edinburgh Handedness Inventory [Oldfield, 1971]. The study was approved by the Research Ethics Board at

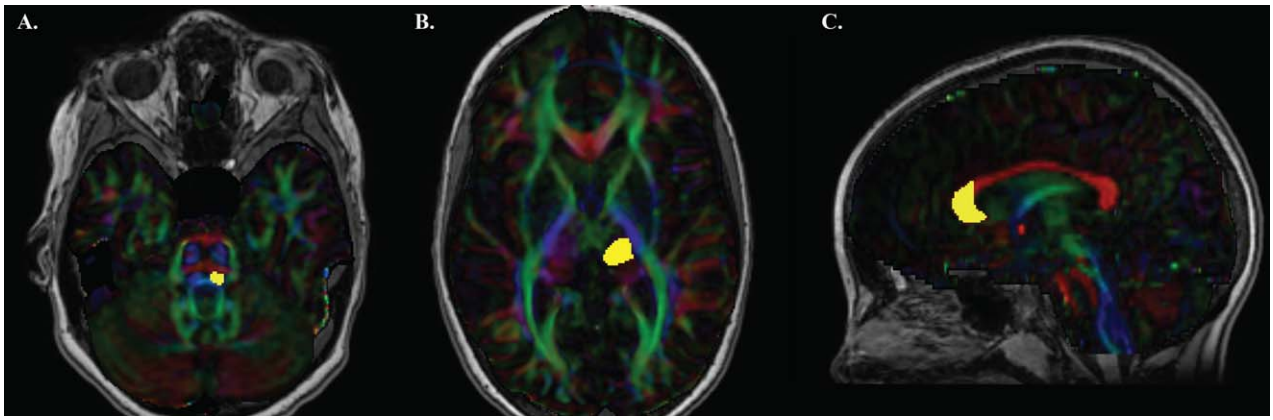

Figure 1.

Regions of interest for generating dorsal column medial lemniscus tracts and anterior forceps. ROIs from the same representative, typically developing 9-year-old are shown. (A) Medial lemniscus (yellow) was placed where the middle cerebellar peduncles (green) and pontine crossing tract (red) were brightest on the color-coded FA map. (B) Ventral posterior lateral (VPL) nucleus of the thalamus (yellow) was placed adjacent to the posterior limb of the internal capsule axially five slices up from the first appearance of the full splenium. (C) Anterior genu of the corpus callosum (yellow) was drawn on a sagittal slice. [Color figure can be viewed at wileyonlinelibrary.com]

the University of Calgary. Written informed consent and assent was obtained.

Imaging Acquisition and Fiber Tracking

Participants were imaged using the Alberta Children's Hospital 3T MRI (GE Discovery MR750w, GE Healthcare, Waukesha, WI) using a 32-channel receive-only head coil (MR Instruments). A fast spoiled gradient echo sequence obtained high-resolution T1-weighted anatomical images with the following parameters: 166 slices, repetition time (TR) = 8.5 ms, echo time (TE) = 3.2 ms, flip angle = 11, field of view = 256, matrix size = 256 × 256, axial acquisition, voxels = 1 mm^3 isotropic. A DTI sequence was acquired using: 32 directions, TR = 11.5 s, TE = 69.1 ms, b-values = 0, 750 s/mm^2; matrix size = 256 × 256, voxels = 2.2 mm^3 isotropic, and scan duration = 6:13 minutes. FSL's Diffusion Toolbox (FDT) was used to correct for eddy current distortions and subject movement in each participant's DWI, followed by the calculation of the diffusion tensor and maps of fractional anisotropy (FA), mean diffusivity (MD), radial (RD), and axial (AD) diffusivity. Images were visually inspected for artifacts.

Probabilistic tractography of DCML sensory tracts was performed using MRtrix software (FA threshold = 0.2, angle 70°, 7,500 streamline samples) [Tournier et al., 2012]. A two region of interest (ROI) approach required streamlines to travel through both the medial lemniscus and ventral posterior lateral (VPL) nucleus of the thalamus. Seed regions were manually defined on color-coded FA maps at anatomically guided locations according to known anatomy (Fig. 1A, B) [Habas and Cabanis, 2007; Mori et al., 2008; Oishi et al., 2011]. ROIs were drawn on the color-coded FA maps containing directional information more accurate than the T1 anatomical image to better resolve the position of the VPL thalamus. Spurious fibers from the corpus callosum and cerebellum were identified and removed from the principal sensory tracts. No other trimming was done. In both hemispheres, mean FA, MD, RD, AD, and fiber count was calculated from the entire tract. The DCML tract in the stroke-affected hemisphere was classified as the tract in the non-dominant hemisphere, while the unaffected hemisphere was classified as the dominant hemisphere in stroke cases. In our right-handed controls, the DCML tract in the right hemisphere was classified as the tract in the non-dominant hemisphere, while the tract in the left hemisphere was referred to as the dominant DCML tract. Intra-class correlations (ICC) evaluated intra-rater reliability and were calculated using FA, MD, RD, and AD values from repeat tractography analysis performed by the same blinded investigator on 14 randomly selected participants with at least 2 weeks between sessions.

To demonstrate the specificity of our DCML tract measures and their relationship with robotic proprioceptive measures, we generated the anterior forceps tract in all 50 of our participants. Using MRtrix software (FA threshold = 0.2, angle 70°, 7,500 streamline samples) [Tournier et al., 2012], we placed the crosshairs of the cursor axially on the middle of the genu and switched to the sagittal view. One ROI of the anterior portion of the corpus callosum was manually defined on the color-coded FA map based on a previous study of segmentation of the corpus callosum (Fig. 1C) [Hofer and Frahm, 2006]. Fibers from the cingulum were identified and excluded from the

overall tract. From the tract generated the mean FA, MD, RD, AD, and fiber count was calculated.

A custom group T1 template was created for healthy controls using Advanced Normalization Tools (ANTs) [Avants et al., 2011]. Normalization of participant brains to the custom T1 template was performed in order for sensory tracts to be overlaid in a common space. SyN symmetric diffeomorphic deformation fields were calculated to transform each participant's T1 anatomical image into the T1 template space. These transformations preserve topology and have been shown to be particularly effective in both normal [Klein et al., 2009] and neurodegenerative [Avants et al., 2008] populations. These same deformation fields were applied to the sensory tract masks to enable spatial comparisons in a common space. Visual inspection was performed at each step to ensure that the warping was accurate and that the stroke lesions were not excessively deformed. Group sensory tract maps (AIS, PVI, controls) were generated by overlaying the tracts in each hemisphere. Degree of overlap of each tract was quantified using a Dice coefficient (similar to a Jaccard index) in relation to one exemplar control using in-house Matlab scripts (Mathworks, Natick, MA). Dice coefficients (DC) compared the similarity of overlap between participants and the exemplar control and were calculated as follows: $DC = (A \cap B)/(A \cup B)$ where A is the voxel mask for the exemplar voxel (from a representative typically developing control subject) and B is the voxel mask for comparison [Dice, 1945]. Larger Dice similarity coefficients indicated a greater extent of voxel overlap in three dimensions.

Robotic Assessment of Proprioception

Assessments were performed at the Foothills Medical Centre Stroke Robotics Laboratory (Calgary, Canada). A KINARM robotic exoskeleton (BKIN Technologies Ltd., Kingston, Ontario) assessed position sense [Dukelow et al., 2010; Kuczynski et al., 2016] and kinesthesia [Semrau et al., 2013; Kuczynski et al., 2016, under review], as described previously. The robot supported the arms in the horizontal plane with visual feedback via a horizontally mounted display (Fig. 2A). The device was custom-fit for each participant including risers for the arm troughs and a booster seat with foam padding for optimal limb positioning in smaller children. Participants completed the position-matching and kinesthesia tasks twice: first with the vision of the upper extremities occluded by an apron and shutter, and subsequently with vision restored. For controls, the robot moved the participant's dominant arm and the subject matched with their non-dominant arm.

For the position-matching task, participants sat comfortably in the modified wheelchair base with elbows flexed. The robot moved the stroke-affected, non-dominant limb (passive arm) to one of nine spatial targets separated by 6 cm. Participants were required to mirror-match the final position with the opposite arm (Fig. 2B). Each participant completed a total of six blocks of trials where the order of the nine targets was pseudo-randomized for a total of 54 movements. The primary outcome was trial-to-trial variability (Var_{xy}) of hand position-matched by the unaffected arm compared with the robot movement in centimeters. Secondary outcomes included the area contracted or expanded of the workspace matched by the unaffected arm ($Area_{xy}$) and differences in spatial hand position ($Shift_{xy}$) between the two arms as measured in centimeters [Dukelow et al., 2010; Herter et al., 2014; Kuczynski et al., 2016].

For the kinesthesia task, the robot moved the stroke-affected or non-dominant arm to one of three spatial locations separated by 12 cm with a speed of 0.18 m/s. As soon as the participant felt the robot move, they were required to mirror-match the sensed amplitude, speed and direction of the robotic movement with their opposite (active) arm (Fig. 2C). Participants completed six blocks of six trials where targets were ordered pseudo-randomly for a total of 36 trials. The following parameters were measured: (1) Response latency (RL): difference in movement onset (the time at which the participant reached 10% of their maximum hand speed) between the active and passive arms measured in milliseconds; (2) Initial direction error (IDE): angular deviation between the active and passive arms at peak hand speed; (3) Peak speed ratio (PSR): ratio of peak hand speed of the active versus passive arm (ratio closer to 1 indicating better matching of passive hand speed); and (4) Path length ratio (PLR): ratio of the distance travelled by the active arm versus the distance travelled by the passive arm (ratio closer to 1 indicating better matching of length). Standard deviation across all trials described the variability in each measure: RL variability (RLv), IDE variability (IDEv), PSR variability (PSRv), and PLR variability (PLRv) [Semrau et al., 2013]. The primary outcome was IDE (and IDEv).

Clinical Assessment

Standardized clinical sensory assessments were performed by the same physiotherapist blinded to stroke type and physiological assessments at the beginning of each session.

A. *Wrist and thumb position sense*. The therapist moved the participant's joint up and down three times with vision occluded. Subjects were required to verbally identify the direction of the end joint position. Outcomes were dichotomized as unable to correctly identify position in either thumb or wrist (0) or able to identify (1).
B. *Thumb localization task (TLT)*. With vision occluded, the therapist moved and positioned the participant's non-dominant upper limb lateral to the midline and asked the participant to pinch their thumb with the thumb and index finger of their opposite hand

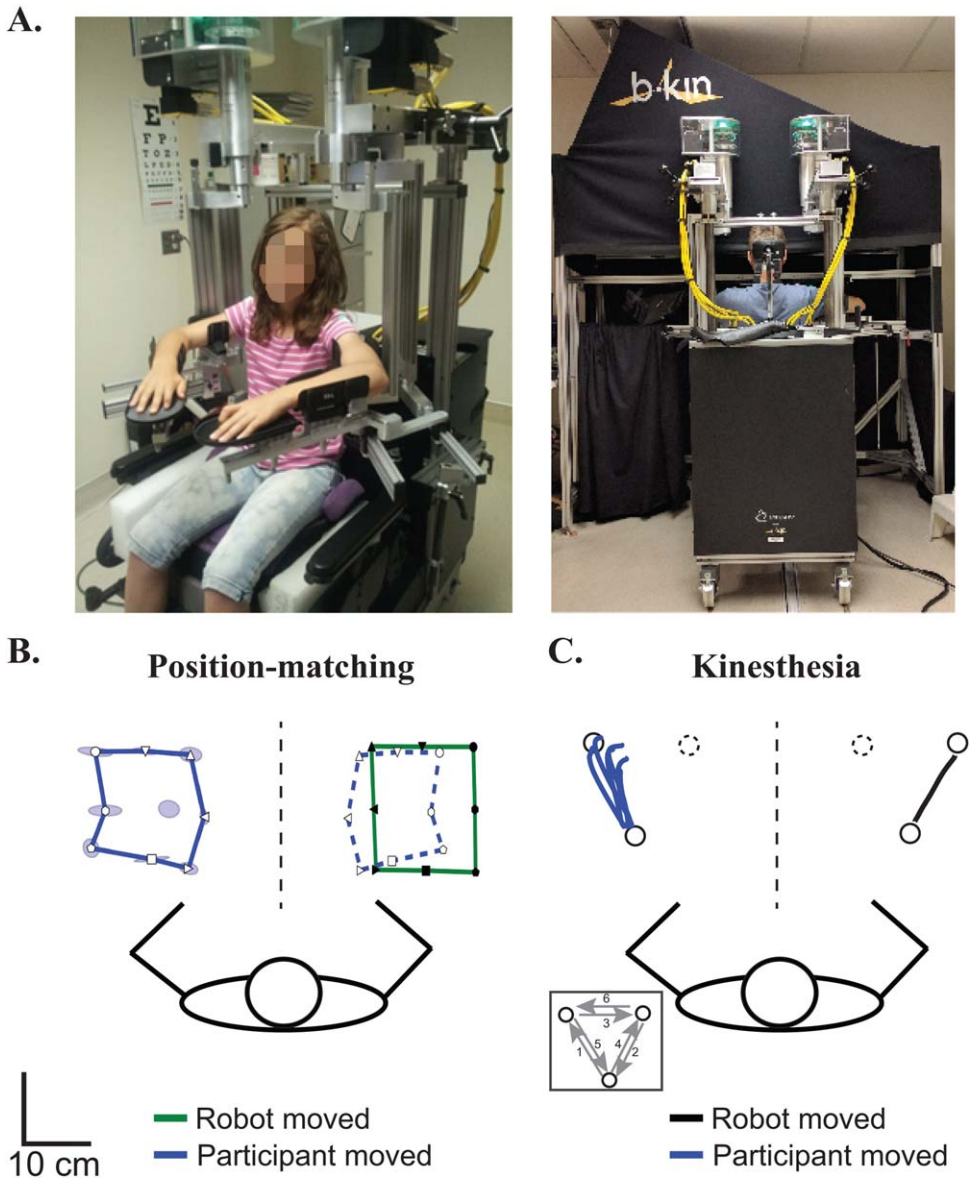

Figure 2.

KINARM robotic exoskeleton and proprioceptive performance. (A) KINARM robot modified for the pediatric population. Modifications included risers and a booster seat for smaller participants. Following custom-fitting, participants were wheeled to the augmented reality workstation to complete proprioceptive tasks. (B) Position-matching performance of an exemplar 11-year-old, right-handed female control. Black symbols in the green lines represent the different positions where the robot moved their right (passive) arm. White symbols in the solid blue lines represent where the participant mirror-matched with their left (active) arm. Blue ellipses around the targets demonstrate the variability (Var_{xy}) of successive matching and represent one standard deviation. For visualization purposes, we have mirrored the participant's active arm performance on top of the robotically moved arm using open symbols and outlining the outer target locations with a blue dashed line. The participant matched the size ($Area_{xy}$) and spatial location ($Shift_{xy}$) of the targets well. (C) Kinesthesia performance of an exemplar 17-year-old, right-handed male control. White circles represent the location of robotic endpoints. The black line shows where the robot moved their right (passive) arm to one position (solid black circle). Blue lines show the six movements made by the participant's left (active) arm to match the movement of the robot in this single direction. [Color figure can be viewed at wileyonlinelibrary.com]

TABLE I. Demographic and clinical details of both upper extremities in stroke cases and controls

	AIS		PVI		Controls	
Number of subjects	14		15		21	
Age (years)	12.0 ± 3.7		12.1 ± 3.3		12.1 ± 3.2	
Sex	5 F, 9 M		6 F, 9 M		9 F, 12 M	
Affected Hemisphere	9 L, 5 R		8 L, 7 R		–	
Handedness	6 L, 8 R		8 L, 7 R		21 R	
	Non-dominant	**Dominant**	**Non-dominant**	**Dominant**	**Non-dominant**	**Dominant**
Position Sense						
Wrist	5 (36%)	3 (21%)	1 (7%)	1 (7%)	0 (0%)	0 (0%)
Thumb	7 (50%)	4 (29%)	1 (7%)	1 (7%)	0 (0%)	0 (0%)
TLT	6 (43%)	0 (0%)	5 (33%)	2 (13%)	0 (0%)	0 (0%)
Stereognosis						
Nickel	8 (57%)	2 (14%)	2 (13%)	1 (7%)	1 (5%)	1 (5%)
Key	9 (64%)	5 (57%)	2 (13%)[a]	2 (7%)[a]	0 (0%)	1 (5%)
Paper clip	9 (64%)	3 (21%)	4 (27%)	2 (7%)	0 (0%)	0 (0%)
Graphesthesia						
7	8 (57%)	2 (14%)	2 (13%)	1 (7%)	1 (5%)	1 (5%)
5	6 (43%)	4 (29%)	2 (13%)	3 (20%)	2 (10%)	2 (10%)
3	5 (57%)	3 (21%)	6 (40%)	0 (0%)	2 (10%)	3 (14%)
Logit AHA [0–100]	68.7 ± 20.7 (37–100)[b]		76.7 ± 15.8 (55–100)[c]		–	
MA [0–100]	78.7 ± 18.1 (52–100)[b]		89.5 ± 11.1 (64–100)[c]		–	

Participant age is indicated as a mean ± standard deviation. Results from Position Sense, Thumb Localization Test (TLT), Stereognosis, and Graphesthesia are shown as the number of subjects who failed the task. Assisting Hand Assessment (AHA) and Melbourne Assessment of Unilateral Upper Limb Function (MA) scores are shown as a mean ± standard deviation with the range of scores (round brackets). Abbreviations: arterial ischemic stroke (AIS), periventricular venous infarction (PVI), female (F), male (M), L (left), R (right).
[a]Indicates data missing from one subject.
[b]Indicates data missing from two subjects.
[c]Indicates data missing from three subjects.

[Hirayama et al., 1999]. The task was scored on a scale from 0 (no difficulty locating) to 3 (unable to locate). Outcomes were dichotomized as normal (0) or impaired (>0).

C. *Stereognosis*. With vision occluded, standardized objects (nickel, key, and paper clip) were sequentially placed in the palm bilaterally, starting with the non-dominant hand. Participants were asked to verbally identify the object and scored 0 (unable to identify), 0.5 (identified the category but not the object), or 1 (able to identify). Scores were dichotomized as impaired (0) if unable to correctly identify 2 or more objects, or normal (1).

D. *Graphesthesia*. With vision occluded, the back of a pen was used to "draw" a 3, 5, and 7 in the palm bilaterally, starting with the non-dominant hand. Participants verbally identified the number and scored either 0 (unable to identify) or 1 (able to identify). Scores were dichotomized as normal (1) or impaired (0) if unable to correctly identify 2 or more numbers.

Standardized, validated assessments of sensorimotor function to assess bimanual upper extremity function were:

A. *Assisting Hand Assessment* (AHA), a 22-item assessment measuring bimanual hand function [Krumlinde-sundholm et al., 2007; Krumlinde-sundholm and Eliasson, 2003] quantified using logit AHA units ranging from 37 (little to no use of impaired hand) to 100 (normal motor function).

B. *Melbourne Assessment of Unilateral Upper Limb Function* (MA), a 16-task measure of unilateral upper limb motor function [Bourke-Taylor, 2003; Randall et al., 1999] with scores ranging from 0 (inability to perform tasks) to 100 (no difficulty performing tasks).

Statistical Analysis

Kolmogorov–Smirnov tests evaluated normality of data distribution. A one-way, mixed model analysis of covariance (ANCOVA) with Bonferroni post-hoc correction tested for significant differences among the three subject groups for diffusion parameters in each hemisphere while controlling for age. Paired *t*-tests evaluated differences of diffusion parameters between hemispheres within each

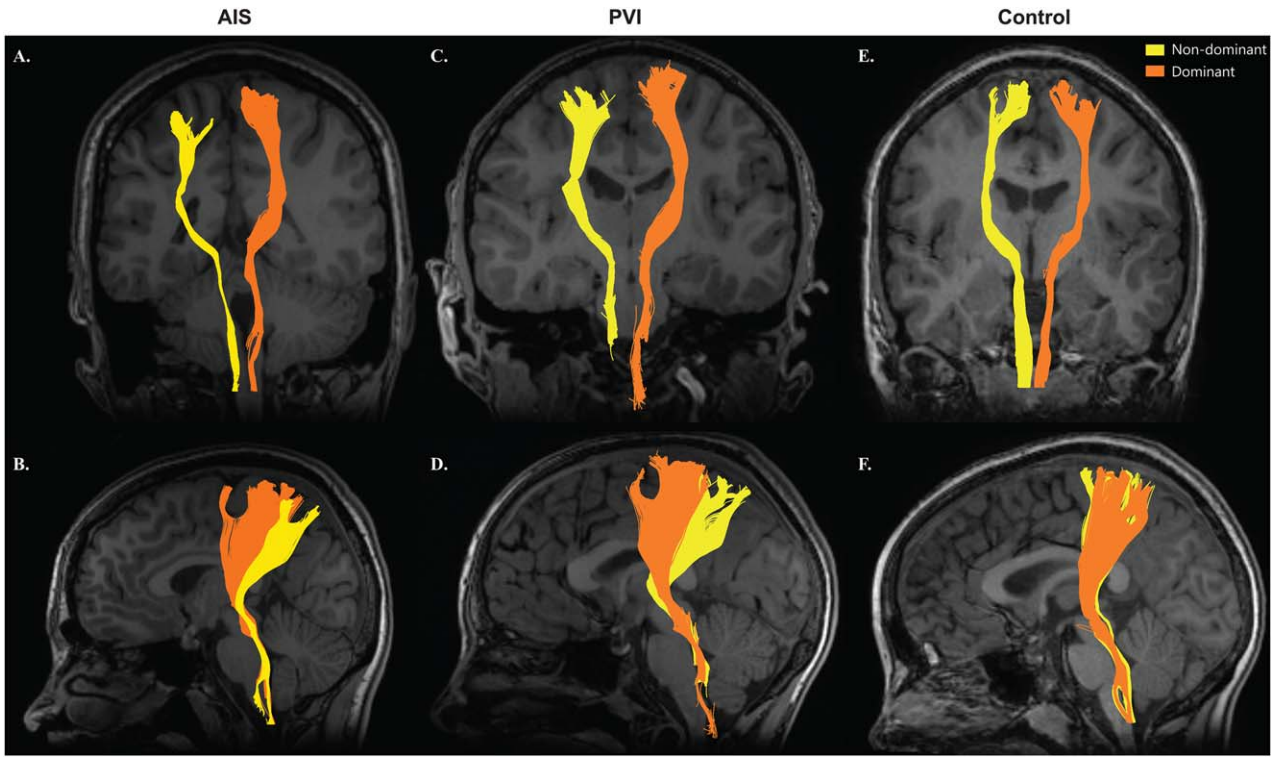

Figure 3.

DCML tracts. DCML sensory tracts of an AIS (A, B), PVI (C, D), and healthy control (E, F) participant. Non-dominant tracts (yellow) were displaced laterally and posteriorly relative to the dominant tracts (orange) in the AIS (B) and PVI (D) participants. Each participant was within the normal range (two standard deviations from the mean) of fiber count in their respective group. [Color figure can be viewed at wileyonlinelibrary.com]

group. An ANCOVA with Bonferroni post-hoc correction evaluated the difference between the robotic performances of all three groups while controlling for the effects of age. The relationship between robotic position sense and kinesthesia measures (no vision condition) with DTI parameters was assessed using partial Spearman's correlations controlling for age. A Bonferroni post-hoc test corrected for multiple comparisons (new alpha = 0.005). Ratios of $Area_{xy}$, PSR, and PLR were generated by comparing raw values to the median to create one-sided measures. Chi-square tests assessed associations between clinical sensorimotor function and diffusion measures. The developmental trajectories of DTI parameters with age were fitted with quadratic and linear equations based on R squared value. Statistical analyses were performed using SigmaPlot (Systat Software Inc., San Jose, CA), SPSS (IBM, Armonk, NY), and Matlab (Mathworks, Natick, MA) software.

RESULTS

A total of 54 participants were recruited: 21 controls, 18 AIS, and 15 PVI. Four AIS cases were excluded due to inability to generate sensory tracts in their lesioned hemisphere due to extensive white matter damage. The final sample of 50 included 21 controls, 14 AIS, and 15 PVI. Demographic and clinical features of the participants are shown in Table I. Intra-rater reliability was high (ICC > 0.93, $P < 0.001$) for FA, MD, RD, and AD, and moderate (ICC > 0.81, $P < 0.001$) for fiber count.

Sensory tracts for a participant from each group are depicted in Figure 3. Tracts in the lesioned, non-dominant hemisphere for AIS and PVI were often displaced laterally and posteriorly. Mean tract overlap was greatest in the AIS group compared with controls in both the non-dominant ($DC = 0.037 \pm 0.03$ versus 0.18 ± 0.2, $P < 0.01$) and dominant ($DC = 0.062 \pm 0.047$ vs. 0.21 ± 0.19, $P < 0.01$) hemispheres. Tracts in the PVI group looked similar to controls but with less density in both the non-dominant ($DC = 0.081 \pm 0.04$ vs. 0.18 ± 0.2, $P = 0.07$) and dominant ($DC = 0.15 \pm 0.05$ vs. 0.21 ± 0.19, $P = 0.07$) hemispheres.

Non-Dominant Hemisphere DCML Diffusion Parameters

All five white matter parameters of the non-dominant hemisphere correlated with age in the control group: FA

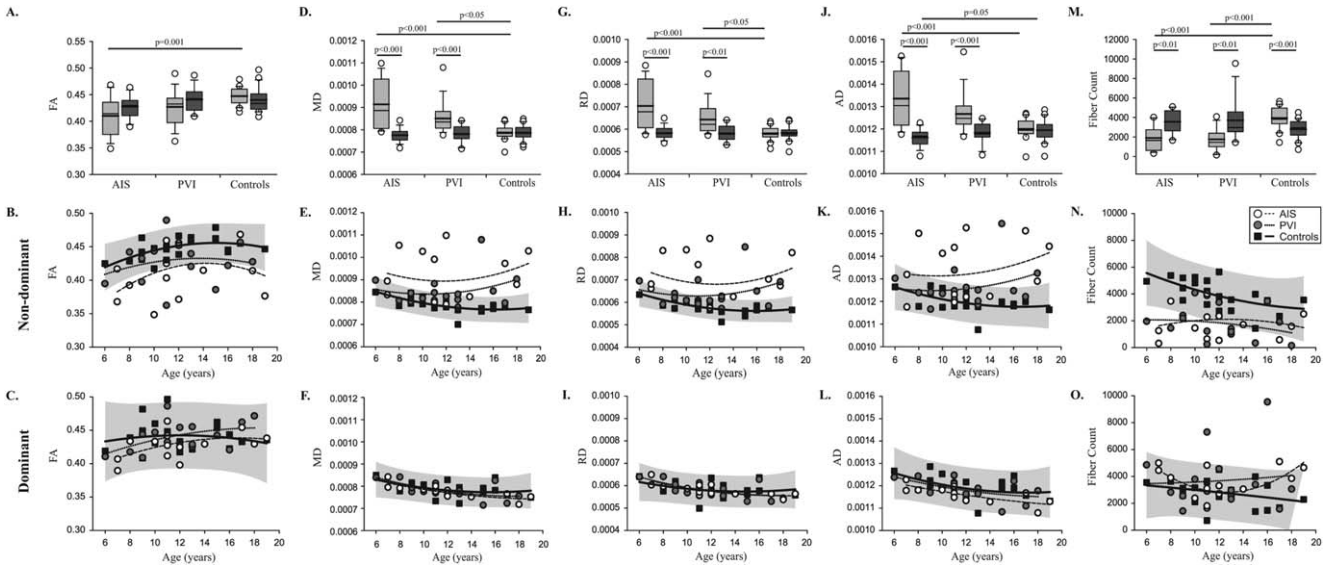

Figure 4.

Diffusion parameters of sensory tracts in cases and controls. Fractional anisotropy (FA) (A–C), mean diffusivity (MD) (D–F), radial (RD) (G–I), and axial (AD) diffusivity (J–L), and fiber count (M–O) are shown. Boxplots of diffusion parameters (top row) of non-dominant (light gray bars) and dominant (dark gray bars) hemispheres are shown for each of the three groups. Scatter plots for the non-dominant (middle row) and dominant (bottom row) hemisphere diffusion measures show the stroke cases and controls with 95% prediction intervals of control performance defining normal boundaries (light gray box).

($R = 0.45$, $P < 0.05$), MD ($R = -0.58$, $P < 0.01$), RD ($R = -0.60$, $P < 0.01$), AD ($R = -0.48$, $P < 0.05$), and fiber count ($R = -0.60$, $P < 0.01$).

Compared with healthy controls, non-dominant tract mean FA was lower in the AIS group ($F(2,46) = 7.91$, $P = 0.001$; 0.41 ± 0.04 vs. 0.45 ± 0.02) but not in PVI (0.43 ± 0.03, $P = 0.1$) (Fig. 4A). Eight (57%) AIS and six (40%) PVI participants fell outside the normal range of FA in the non-dominant hemisphere (95% prediction interval of controls) (Fig. 4B). MD was greater in both AIS ($9.14 \times 10^{-4} \pm 1.1 \times 10^{-4}$, $P < 0.001$) and PVI ($8.51 \times 10^{-4} \pm 7.1 \times 10^{-5}$, $P = 0.04$) cases relative to controls ($F(2,46) = 12.5$, $P < 0.001$; $7.87 \times 10^{-4} \pm 3.1 \times 10^{-5}$; Fig. 4D). Seven (50%) AIS and six (40%) PVI subjects fell outside the 95% prediction interval MD of controls (Fig. 4E).

Mean RD was greater in stroke cases compared with controls ($F(2,46) = 12.9$, $P < 0.001$). Both AIS ($7.04 \times 10^{-4} \pm 1.0 \times 10^{-4}$, $P < 0.001$) and PVI ($6.43 \times 10^{-4} \pm 6.7 \times 10^{-5}$, $P = 0.04$) groups showed increased RD relative to controls ($5.81 \times 10^{-4} \pm 2.8 \times 10^{-5}$; Fig. 4G). Nine (64%) AIS and six (40%) PVI participants fell outside the 95% prediction intervals normal RD of controls (Fig. 4H). The AIS group demonstrated greater AD compared with healthy controls ($F(2,46) = 9.66$, $P < 0.001$; $1.33 \times 10^{-3} \pm 1.3 \times 10^{-4}$ vs. $1.20 \times 10^{-3} \pm 4.2 \times 10^{-5}$; Fig. 4J). Seven (50%) AIS and three (21%) PVI fell outside the normal range of control AD (Fig. 4K).

Fiber count was lower in AIS ($1{,}898 \pm 1{,}198$) and PVI ($1{,}757 \pm 1{,}152$) compared with controls ($3{,}942 \pm 1{,}082$; $F(2,46) = 21.7$, $P < 0.001$; Fig. 4M). Six (43%) AIS and eleven (73%) PVI participants fell outside the prediction intervals of fiber count of 95% of controls (Fig. 4N). Control fiber count correlated with FA ($R = -0.67$, $P < 0.01$), MD ($R = 0.54$, $P = 0.01$), and RD ($R = 0.63$, $P < 0.01$). No differences in the diffusion properties of the lesioned hemisphere were observed between AIS and PVI groups.

Dominant Hemisphere DCML Diffusion Parameters

In the dominant hemisphere, MD correlated with age in both the AIS ($R = -0.80$, $P = 0.001$) and PVI ($R = -0.63$, $P = 0.01$) group. RD was correlated with age in the AIS ($R = -0.75$, $P < 0.01$) and PVI ($R = -0.61$, $P < 0.05$) groups. AD in the dominant hemisphere correlated with age in the AIS ($R = -0.71$, $P < 0.01$), PVI ($R = -0.53$, $P < 0.05$), and control ($R = -0.44$, $P < 0.05$) groups. All diffusion variables were comparable between the dominant (contralesional) hemisphere in stroke participants and controls (Fig. 4).

DCML Diffusion Differences Between Hemispheres

Mean, radial, and axial diffusivities, and fiber count were significantly lower in the lesioned, non-dominant hemisphere of the AIS and PVI groups relative to the

TABLE II. Robotic proprioceptive performance

	AIS		PVI		Controls	
Position sense	No vision	Vision	No vision	Vision	No vision	Vision
Var_{xy} (cm)	$5.70 \pm 2.2^{+}$	$4.19 \pm 1.6^{\dagger}$	$5.39 \pm 2.0^{+}$	$4.07 \pm 1.4^{+}$	3.38 ± 1.0	2.57 ± 0.64
	7 (50%)	8 (57%)	7 (47%)	7 (47%)	1 (0.6%)	1 (0.6%)
$Area_{xy}$	0.56 ± 0.3	0.62 ± 0.3	0.95 ± 0.6	0.85 ± 0.4	0.70 ± 0.2	0.75 ± 0.1
	5 (36%)	4 (29%)	6 (40%)	7 (47%)	0 (0%)	0 (0%)
$Shift_{xy}$ (cm)	$8.88 \pm 8.1^{+}$	$9.27 \pm 7.4^{+}$	4.99 ± 2.7	5.01 ± 2.7	3.93 ± 1.9	3.96 ± 2.4
	6 (43%)	4 (29%)	1 (7%)	2 (13%)	1 (0.6%)	1 (0.6%)
Kinesthesia	No vision	Vision	No vision	Vision	No vision	Vision
RL (s)	$0.53 \pm 0.2^{+}$	$0.53 \pm 0.2^{\dagger}$	0.48 ± 0.2*	0.47 ± 0.2*	0.34 ± 0.1	0.33 ± 0.1
	8 (57%)	7 (50%)	5 (33%)	3 (20%)	2 (1%)	1 (0.6%)
RLv (s)	$0.30 \pm 0.1^{+}$	$0.26 \pm 0.1^{+}$	0.24 ± 0.1*	0.23 ± 0.2*	0.15 ± 0.1	0.12 ± 0.07
	6 (43%)	7 (50%)	3 (20%)	4 (27%)	2 (1%)	1 (0.6%)
IDE (°)	$40.6 \pm 14^{\dagger}$	$32.3 \pm 12^{\dagger}$	30.5 ± 8.0*	$26.8 \pm 8.7^{+}$	21.4 ± 6.0	16.3 ± 5.6
	10 (71%)	8 (57%)	6 (40%)	6 (40%)	0 (0%)	1 (0.6%)
IDEv (°)	$32.7 \pm 12^{\dagger}$	$29.2 \pm 11^{\dagger}$	$28.0 \pm 9.8^{+}$	$25.4 \pm 11^{+}$	16.8 ± 5.8	14.4 ± 6.3
	10 (71%)	5 (36%)	8 (53%)	4 (27%)	1 (0.6%)	2 (1%)
PSR	1.17 ± 0.32	1.12 ± 0.16	1.20 ± 0.24	1.16 ± 0.19	1.10 ± 0.11	1.07 ± 0.093
	4 (29%)	4 (29%)	5 (33%)	5 (33%)	0 (0%)	1 (0.6%)
PSRv	$0.53 \pm 0.2^{\dagger}$	$0.49 \pm 0.1^{\dagger}$	$0.48 \pm 0.2^{+}$	$0.42 \pm 0.2^{+}$	0.31 ± 0.1	0.25 ± 0.072
	9 (64%)	9 (64%)	10 (67%)	6 (40%)	0 (0%)	1 (0.6%)
PLR	1.22 ± 0.37*	1.16 ± 0.22*	1.15 ± 0.22	1.09 ± 0.17	1.02 ± 0.091	1.00 ± 0.086
	5 (36%)	5 (36%)	6 (40%)	4 (27%)	0 (0%)	1 (0.6%)
PLRv	$0.51 \pm 0.2^{\dagger}$	$0.43 \pm 0.2^{\dagger}$	$0.38 \pm 0.1^{+}$	0.32 ± 0.1*	0.22 ± 0.06	0.21 ± 0.08
	10 (71%)	7 (50%)	11 (73%)	4 (27%)	0 (0%)	1 (0.6%)

Scores are shown as mean ± standard deviation. The number of participants in each group that failed the parameter is shown. Statistical significance in performance compared with controls is indicated as: * $P < 0.05$; $^{+}$ $P < 0.01$; † $P < 0.001$.

dominant hemisphere ($P < 0.01$). Interestingly, fiber count in the non-dominant hemisphere of controls was significantly greater than the dominant hemisphere ($P < 0.001$). Overall, FA and fiber count increased progressively with age, while mean, radial, and axial diffusivities decreased with age in all three groups (Fig. 4).

Robotic Proprioception and Sensory Tractography Measures

Position-matching performance differed between stroke cases and controls as previously described (Table II). The AIS group was more impaired and had greater $Area_{xy}$ ($P = 0.01$) without vision, and $Shift_{xy}$ ($P = 0.04$) with vision than the PVI group. Diffusion measures of the lesioned, non-dominant hemisphere correlated with variability (Var_{xy}), but neither $Area_{xy}$ nor $Shift_{xy}$ (Table III). Robotic Var_{xy} was moderately correlated with all diffusion measures of the non-dominant hemisphere: FA ($R = -0.41$, $R^2 = 0.16$, $P < 0.005$; Fig. 4A,B), MD ($R = 0.54$, $R^2 = 0.29$, $P < 0.005$), RD ($R = 0.54$, $R^2 = 0.29$, $P < 0.005$), AD ($R = 0.51$, $R^2 = 0.26$, $P < 0.005$), and fiber count ($R = -0.48$, $R^2 = 0.23$, $P < 0.005$).

Kinesthetic performance was impaired in stroke cases compared with controls in all eight parameters as described previously (Table II). Compared with the PVI group, participants with AIS had greater initial direction error (IDE) when vision was occluded ($P = 0.02$). DCML diffusion parameters of the lesioned hemisphere correlated with most kinesthetic measures (Table III). IDE was moderately correlated with fiber count ($R = -0.44$, $R^2 = 0.19$, $P < 0.005$) of the non-dominant hemisphere, but not FA ($R = -0.29$, $R^2 = 0.084$, $P = 0.4$; Fig. 4C,D). Initial direction error variability (IDEv) was negatively correlated with fiber count ($R = -0.46$, $R^2 = 0.21$, $P = 0.001$) in the non-dominant hemisphere (Table III). In the dominant hemisphere, no diffusion measures of the DCML tract correlated with kinesthetic parameters (Table 5; Fig. 5).

Association Between Clinical Sensorimotor Function and Tractography Measures

AHA scores did not correlate with the average FA in the lesioned, non-dominant hemisphere in the AIS group ($R = 0.57$, $R^2 = 0.32$, $P = 0.05$) nor in PVI ($R = -0.024$, $R^2 = 5.8 \times 10^{-4}$, $P = 0.9$) following correction for multiple comparisons. AHA scores correlated with the average MD

TABLE III. Relationship between robotic measures of proprioception and DCML DTI parameters

	Non-dominant hemisphere	Dominant hemisphere
Position sense		
Var_{xy} (cm)		
FA	$R = -0.406$, $P = 0.004$*	$R = -0.171$, $P = 0.241$
MD	$R = 0.540$, $P = 6.20 \times 10^{-5}$*	$R = 0.113$, $P = 0.441$
RD	$R = 0.538$, $P = 6.80 \times 10^{-5}$*	$R = 0.222$, $P = 0.125$
AD	$R = 0.510$, $P = 1.83 \times 10^{-4}$*	$R = -0.083$, $P = 0.570$
Fiber Count	$R = -0.483$, $P = 4.45 \times 10^{-4}$*	$R = 0.324$, $P = 0.023$
$Area_{xy}$		
FA	$R = 0.122$, $P = 0.404$	$R = 0.229$, $P = 0.114$
MD	$R = 0.086$, $P = 0.556$	$R = -0.059$, $P = 0.688$
RD	$R = 0.042$, $P = 0.775$	$R = -0.129$, $P = 0.375$
AD	$R = 0.154$, $P = 0.292$	$R = 0.062$, $P = 0.671$
Fiber Count	$R = 0.008$, $P = 0.955$	$R = 0.51$, $P = 0.728$
$Shift_{xy}$ (cm)		
FA	$R = -0.265$, $P = 0.065$	$R = -0.439$, $P = 0.002$*
MD	$R = 0.374$, $P = 0.008$	$R = 0.005$, $P = 0.971$
RD	$R = 0.368$, $P = 0.009$	$R = 0.153$, $P = 0.295$
AD	$R = 0.360$, $P = 0.011$	$R = -0.204$, $P = 0.160$
Fiber Count	$R = -0.235$, $P = 0.104$	$R = 0.215$, $P = 0.138$
Kinesthesia		
RL (s)		
FA	$R = -0.263$, $P = 0.068$	$R = -0.050$, $P = 0.733$
MD	$R = 0.467$, $P = 0.001$*	$R = -0.313$, $P = 0.028$
RD	$R = 0.440$, $P = 0.002$*	$R = -0.205$, $P = 0.159$
AD	$R = 0.482$, $P = 4.57 \times 10^{-4}$*	$R = -0.350$, $P = 0.014$
Fiber Count	$R = -0.270$, $P = 0.061$	$R = 0.118$, $P = 0.421$
RLv (s)		
FA	$R = -0.182$, $P = 0.212$	$R = 0.040$, $P = 0.784$
MD	$R = 0.434$, $P = 0.002$*	$R = -0.223$, $P = 0.124$
RD	$R = 0.394$, $P = 0.005$*	$R = -0.173$, $P = 0.234$
AD	$R = 0.471$, $P = 0.001$*	$R = -0.210$, $P = 0.147$
Fiber Count	$R = -0.181$, $P = 0.214$	$R = 0.243$, $P = 0.093$
IDE		
FA	$R = -0.132$, $P = 0.364$	$R = 0.074$, $P = 0.612$
MD	$R = 0.336$, $P = 0.018$	$R = -0.084$, $P = 0.566$
RD	$R = 0.307$, $P = 0.032$	$R = -0.070$, $P = 0.632$
AD	$R = 0.361$, $P = 0.011$	$R = -0.072$, $P = 0.621$
Fiber Count	$R = -0.437$, $P = 0.002$*	$R = 0.216$, $P = 0.136$
IDEv		
FA	$R = -0.099$, $P = 0.500$	$R = 0.119$, $P = 0.417$
MD	$R = 0.303$, $P = 0.035$	$R = -0.184$, $P = 0.205$
RD	$R = 0.275$, $P = 0.056$	$R = -0.180$, $P = 0.217$
AD	$R = 0.329$, $P = 0.021$	$R = -0.123$, $P = 0.401$
Fiber Count	$R = -0.462$, $P = 0.001$*	$R = 0.201$, $P = 0.166$
PSR		
FA	$R = -0.127$, $P = 0.386$	$R = 0.071$, $P = 0.628$
MD	$R = 0.317$, $P = 0.026$	$R = -0.015$, $P = 0.920$
RD	$R = 0.302$, $P = 0.035$	$R = -0.017$, $P = 0.907$
AD	$R = 0.323$, $P = 0.023$	$R = -0.006$, $P = 0.968$
Fiber Count	$R = -0.283$, $P = 0.049$	$R = 0.044$, $P = 0.762$
PSRv		
FA	$R = -0.269$, $P = 0.062$	$R = 0.063$, $P = 0.666$
MD	$R = 0.531$, $P = 8.80 \times 10^{-5}$*	$R = -0.168$, $P = 0.248$
RD	$R = 0.501$, $P = 2.43 \times 10^{-4}$*	$R = -0.114$, $P = 0.435$
AD	$R = 0.545$, $P = 5.10 \times 10^{-5}$*	$R = -0.182$, $P = 0.210$
Fiber Count	$R = -0.422$, $P = 0.003$*	$R = 0.179$, $P = 0.218$

TABLE III. (continued)

	Non-dominant hemisphere	Dominant hemisphere
Kinesthesia		
PLR		
FA	$R = -0.165$, $P = 0.257$	$R = 0.184$, $P = 0.206$
MD	$R = 0.407$, $P = 0.004$*	$R = -0.134$, $P = 0.360$
RD	$R = 0.381$, $P = 0.007$	$R = -0.171$, $P = 0.239$
AD	$R = 0.423$, $P = 0.002$*	$R = -0.031$, $P = 0.831$
Fiber Count	$R = -0.422$, $P = 0.003$*	$R = -0.024$, $P = 0.867$
PLRv		
FA	$R = -0.236$, $P = 0.103$	$R = 0.138$, $P = 0.344$
MD	$R = 0.416$, $P = 0.003$*	$R = -0.13.$, $P = 0.373$
RD	$R = 0.401$, $P = 0.004$*	$R = -0.131$, $P = 0.370$
AD	$R = 0.416$, $P = 0.003$*	$R = -0.081$, $P = 0.582$
Fiber Count	$R = -0.442$, $P = 0.001$*	$R = 0.067$, $P = 0.648$

Partial Spearman's correlations comparing the relationship between robotic sensory measures (no vision condition) and DCML tract diffusion parameters. R and p-values with age-correction are shown. An asterisks (*) denotes significant correlations following Bonferroni correction for multiple comparisons (new alpha = 0.005). Abbreviations: variability (Var_{xy}), response latency (RL), response latency variability (RLv), initial direction error (IDE), initial direction error variability (IDEv), peak speed ratio (PSR), peak speed ratio variability (PSRv), path length ratio (PLR), path length ratio variability (PLRv), fractional anisotropy (FA), mean diffusivity (MD), radial diffusivity (RD), axial diffusivity (AD).

($R = -0.88$, $R^2 = 0.77$, $P < 0.005$) and RD ($R = -0.74$, $R^2 = 0.55$, $P = 0.005$) in the dominant hemisphere of the AIS group. MA scores were also correlated with mean MD ($R = -0.92$, $R^2 = 0.85$, $P < 0.005$) and AD ($R = -0.74$, $R^2 = 0.55$, $P = 0.005$) in the dominant hemisphere in the AIS group. Clinical measures of sensory function in the stroke-affected and unaffected hand were not associated with DCML diffusion parameters.

Control Tract: Anterior Forceps

The anterior forceps tract was generated for all 50 participants. Mean diffusion measures did not differ between the AIS group and controls. For example, FA was 0.44 ± 0.03 for AIS versus 0.45 ± 0.01 for controls ($P = 1.0$). The only exception was fiber count which was lower in the AIS group ($11{,}953 \pm 3{,}812$) compared with controls ($15{,}376 \pm 2{,}935$, $P < 0.01$). All diffusion measures were comparable between the PVI group and controls. Anterior forceps diffusion measures did not differ between AIS and PVI groups. Robotic proprioceptive measures did not correlate with any diffusion parameters of the anterior forceps (Table IV). Clinical motor scores also did not correlate with the diffusion measures of the anterior forceps.

DISCUSSION

In this study, we characterized the structural connectivity and diffusion properties of DCML white matter pathways in children with perinatal stroke and hemiparetic CP. Compared with controls, children with AIS demonstrated robust differences across all diffusion parameters in the DCML tract in the lesioned, non-dominant hemisphere, while children with PVI showed only moderate differences. Differences in white matter properties were not observed in the dominant hemisphere. Robotic position sense, kinesthetic performance, and functional measures correlated with lesioned DCML diffusion parameters, suggesting altered structural connectivity may in part explain proprioceptive disability that is clinically relevant.

Aside from motor disabilities, perinatal brain injury causes disturbances in sensation and perception that may contribute to functional disability [Bax et al., 2005; Bleyenheuft and Gordon, 2013; de Campos et al., 2014]. Studies in children with CP have reported impairments in touch threshold [Hoon et al., 2009], proprioception [Hoon et al., 2009], tactile discrimination [Auld et al., 2012], and stereognosis [Tizard et al., 1954; Van Heest et al., 1993]. However, the study of sensory dysfunction in CP has been hampered by a lack of objective, accurate assessment tools. We believe that our study makes three important advances in studying proprioceptive dysfunction in children with perinatal stroke. Using robotic technology, we have previously demonstrated the sensitivity and specificity of the KINARM robot in quantifying position sense [Kuczynski et al., 2016] and kinesthesia [Kuczynski et al., 2016, in revision] in school-aged children with and without disability. Secondly, we have quantified the diffusion properties of the DCML pathway using diffusion tensor imaging (DTI) and shown differences in the white matter diffusion properties of these tracts in children with arterial and venous perinatal ischemic strokes. Our findings show that the diffusion measures of the DCML tracts in the lesioned,

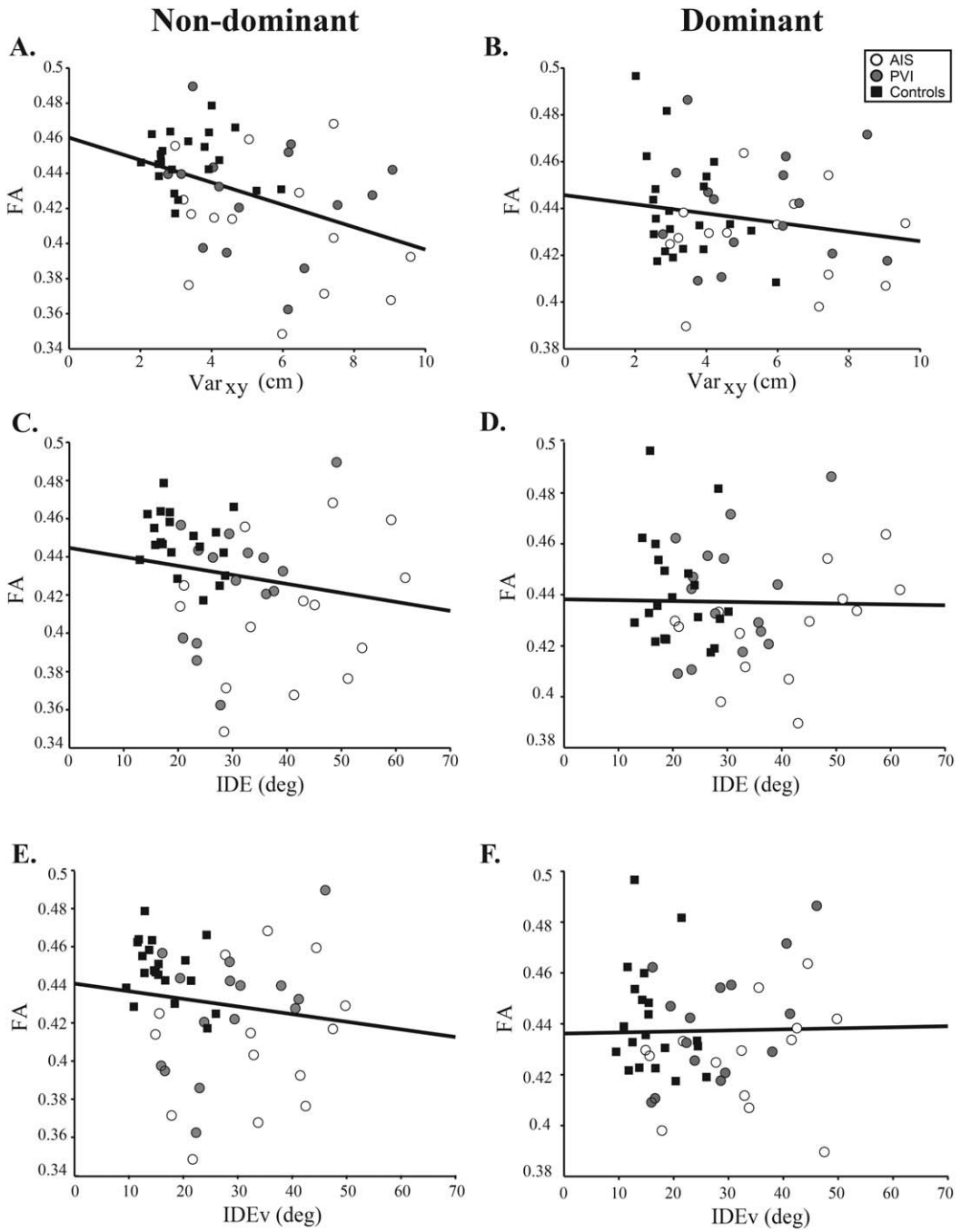

Figure 5.

FA versus robotic proprioception. Scatter plots for the non-dominant and dominant hemisphere diffusion measures show the stroke cases and controls with fitted regression line. Var_{xy} (A, B) was moderately correlated with non-dominant hemisphere FA ($R = -0.41$, $R^2 = 0.17$, 95% CI_{FA}: -0.65, -0.19, $P < 0.005$) but not FA in the dominant hemisphere ($R = -0.17$, $R^2 = 0.029$, 95% CI_{FA}: -0.47, 0.22, $P = 0.2$). Kinesthetic IDE (C, D) did not correlate with non-dominant FA ($R = -0.13$, $R^2 = 0.017$, 95% CI_{FA}: -0.45, 0.24, $P = 0.4$) nor in the dominant hemisphere ($R = 0.0074$, $R^2 = 5.5 \times 10^{-5}$, 95% CI_{FA}: -0.19, 0.41, $P = 0.6$). IDEv (E, F) did not correlate with non-dominant FA ($R = -0.099$, $R^2 = 9.8 \times 10^{-3}$, 95% CI_{FA}: -0.48, 0.25, $P = 0.5$) nor dominant hemisphere FA ($R = 0.12$, $R^2 = 0.014$, 95% CI_{FA}: -0.14, 0.37, $P = 0.4$).

TABLE IV. Relationship between the anterior forceps diffusion parameters and robotic measures of proprioception

	FA	MD	RD	AD	Fiber Count
Position sense					
Var_{xy} (cm)	$R=-0.004$, $P=0.978$	$R=-0.111$, $P=0.447$	$R=-0.067$, $P=0.649$	$R=-0.160$, $P=0.273$	$R=-0.297$, $P=0.038$
$Area_{xy}$	$R=0.420$, $P=0.003$	$R=-0.264$, $P=0.067$	$R=-0.348$, $P=0.014$	$R=-0.023$, $P=0.876$	$R=0.417$, $P=0.003$
$Shift_{xy}$ (cm)	$R=-0.228$, $P=0.116$	$R=0.343$, $P=0.016$	$R=0.346$, $P=0.015$	$R=0.230$, $P=0.111$	$R=-0.268$, $P=0.063$
Kinesthesia					
RL (s)	$R=-0.044$, $P=0.765$	$R=0.037$, $P=0.803$	$R=0.054$, $P=0.714$	$R=-0.007$, $P=0.960$	$R=-0.364$, $P=0.010$
RLv (s)	$R=0.114$, $P=0.437$	$R=0.008$, $P=0.957$	$R=-0.033$, $P=0.821$	$R=0.082$, $P=0.574$	$R=-0.069$, $P=0.638$
IDE (°)	$R=-0.138$, $P=0.345$	$R=-0.104$, $P=0.478$	$R=-0.014$, $P=0.924$	$R=-0.239$, $P=0.098$	$R=-0.208$, $P=0.151$
IDEv (°)	$R=-0.066$, $P=0.650$	$R=-0.075$, $P=0.609$	$R=-0.020$, $P=0.890$	$R=-0.154$, $P=0.291$	$R=-0.188$, $P=0.195$
PSR	$R=-0.173$, $P=0.235$	$R=-0.036$, $P=0.807$	$R=0.054$, $P=0.713$	$R=-0.193$, $P=0.184$	$R=-0.128$, $P=0.380$
PSRv	$R=-0.052$, $P=0.723$	$R=-0.073$, $P=0.620$	$R=-0.012$, $P=0.935$	$R=-0.164$, $P=0.261$	$R=-0.358$, $P=0.012$
PLR	$R=-0.122$, $P=0.404$	$R=-0.154$, $P=0.291$	$R=-0.048$, $P=0.744$	$R=-0.304$, $P=0.034$	$R=-0.182$, $P=0.211$
PLRv	$R=0.028$, $P=0.850$	$R=-0.241$, $P=0.096$	$R=-0.171$, $P=0.239$	$R=-0.295$, $P=0.040$	$R=-0.221$, $P=0.126$

Partial spearman's correlations comparing the relationship between robotic sensory measures (no vision condition) and the diffusion parameters of the anterior forceps. Correlations were corrected for multiple comparisons (new $\alpha = 0.005$). Abbreviations: variability (Var_{xy}), response latency (RL), response latency variability (RLv), initial direction error (IDE), initial direction error variability (IDEv), peak speed ratio (PSR), peak speed ratio variability (PSRv), path length ratio (PLR), path length ratio variability (PLRv), fractional anisotropy (FA), mean diffusivity (MD), radial diffusivity (RD), axial diffusivity (AD). An asterisks (*) denotes significant correlations.

stroke-affected hemisphere of these patients does not follow the developmental curve of typically developing children. Finally, we have shown that these moderate differences in diffusion parameters in the lesioned DCML tract are associated with robotic proprioceptive performance.

Lesions to the sensorimotor cortex or subcortical white matter cause abnormalities in posture, muscle tone, range of movement, and spasticity that result in disability for children with CP [Chang et al., 2009; Hoon et al., 2002; Nagae et al., 2007]. This damage may affect the development of cortical and thalamic regions critical for sensory processing [Tsao et al., 2014]. Previous diffusion MRI studies have described the association between structural connectivity of the descending corticospinal tracts [van der Aa et al., 2013; Kirton et al., 2007; Lennartsson et al., 2015; Roze et al., 2012; Yoshida et al., 2010] and posterior thalamic radiations [Hoon et al., 2009] with clinical function in hemiparetic CP. Many found that reduced FA and increased MD in lesioned tracts was negatively correlated with clinical function including the measures employed here (AHA, MA) [Rose et al., 2011; Tsao et al., 2013]. Changes in diffusion properties of the motor tracts appear comparable to those that we observed here in the lesioned DCML tracts. Reduced FA has been associated with a loss of uniformity of axonal fibers [Basser and Pierpaoli, 1996], whereas increases in RD and MD may be consistent with reduced myelination and tract density respectively [Mori and Zhang, 2006; Song et al., 2002]. These findings suggest a disruption in axonal organization and density, with a corresponding loss of ordered diffusion in the lesioned sensory tracts following perinatal stroke, though pathological studies would be required to confirm this.

In the PVI group, differences in the diffusion measures of the non-dominant sensory tracts were more modest but also demonstrated greater mean and radial diffusivities compared with controls. The lack of FA and AD differences in PVI may suggest relatively greater structural preservation of sensory tract fibers reaching the post-central gyrus compared with children with AIS. Additionally, multimodal imaging studies have shown reorganization following early brain injury where the ascending thalamocortical pathways may bypass subcortical PVI lesions and ultimately reach the somatosensory cortex [Nevalainen et al., 2012; Staudt et al., 2006; Staudt, 2010; Wilke et al., 2008]. Consistent with these findings, we observed that surviving DCML tracts were often organized more posteriorly and laterally in the PVI group compared with controls. On the non-lesioned, dominant side, differences in diffusion parameters between stroke cases and controls were not observed, similar to other studies of thalamocortical projections [Rose et al., 2011], supporting the specificity of the lesioned white matter diffusion changes we observed.

DCML projections in children with AIS and PVI displayed greater differences in sensory tract fiber counts between hemispheres compared with controls. This was expected and is likely attributable to a reduced number of somatosensory fibers in the lesioned, non-dominant hemisphere as a result of stroke-induced damage. This asymmetry was not associated with performance on robotic proprioception tasks or clinical sensory measures, suggesting that sensory tract microstructure (quality) may be more functionally relevant than tract volume (quantity). One study in healthy adults examined DCML tract morphology using the medial lemniscus, VPL thalamus, and

primary somatosensory cortex as seed regions, finding a greater number of voxels in the seed masks of the DCML tract in the non-dominant hemisphere [Jang et al., 2012]. This is consistent with our findings of greater fiber count in the non-dominant hemisphere of our controls. Fiber count also displayed a negative association with age; suggest pruning or other developmental modification.

That our sample spanned a large age range allowed us to assess the maturation of the DCML pathways in children with perinatal stroke compared with typically developing children. Adolescence is an active period of white matter development [Lebel et al., 2008, 2012; Lebel and Beaulieu, 2011], and understanding the potential alteration of white matter tracts caused by perinatal stroke during this time is important. Consistent with previous findings, all three groups showed FA increases and MD, RD, and AD decreases with increasing age. However, our results show that while the dominant hemisphere of hemiparetic children appears to follow a developmental trajectory similar to controls, diffusion measures in the lesioned hemisphere differed from the normative values of the healthy population. These patterns suggest intriguing possibilities that may have implications for rehabilitation planning. It could be that the lesioned hemisphere is not following the expected white matter developmental curve. Alternatively, the typical changes in white matter that occur with maturation may be delayed by the injury (i.e., lagging behind the curve). Through intensive therapy, there may be the potential to change the diffusion properties of the stroke-affected tracts toward more normal developmental curves, possibly improving sensorimotor function. Studies from adult stroke do suggest that diffusion measures [Fan et al., 2015; Wen et al., 2016] and cortical volume [Gauthier et al., 2008] of corticospinal tract connectivity can be changed by intensive therapy. Inclusion of such imaging measures of both motor and sensory tracts before and after intensive rehabilitation in hemiparetic children may carry such utility in the future.

Changes in the lesioned DCML pathway of children with AIS were associated with clinical motor function as measured by standardized assessments. Both the Assisting Hand Assessment and Melbourne Assessment scores were negatively correlated with MD and RD of the dominant hemisphere. These findings suggest that the preservation and or developmental recovery of these primary somatosensory connections likely contribute to overall sensorimotor disability. That clinical assessments specific to sensory function were not related to DTI indices was not surprising as we have previously demonstrated the low sensitivity and specificity of such clinical tests [Kuczynski et al., 2016]. Our findings that sensory tract white matter structural connectivity contributes to disability in perinatal stroke does not preclude the involvement of cortical components of the sensory network. In fact, stronger associations were observed in AIS patients with cortical lesions compared with purely subcortical lesions in the PVI group, suggesting an important role for cortical structures such as the primary somatosensory cortex. Our study cannot distinguish between primary effects of direct injury to the white matter versus secondary degenerative changes that might occur following cortical injury. Integration of other imaging tools in this population may help elucidate the role of cortical sensory processing including resting state functional MRI. Although there have been limited studies to date, task functional MRI offers the potential to define individual cortical reorganization that might then be used a guide for placing ROIs to generate sensorimotor tracts [Walther et al., 2009]. As many hemiparetic children with perinatal stroke have motor control in the contralesional hemisphere, the reorganization of the sensory and motor cortex may also be relevant to clinical function [Kirton, 2013]. Ultimately, the integration of these and other neurophysiological measures to create comprehensive, individualized maps of brain development following early focal injury will advance targeted therapy and personalized medicine in cerebral palsy rehabilitation.

CONCLUSION

Using diffusion tensor imaging, we have characterized the diffusion properties of the DCML pathway in children with perinatal stroke and typically developing controls. The lesioned, stroke-affected hemisphere demonstrated strong differences in the AIS group, and more moderate differences in the PVI group, relative to controls. Robotic measures of proprioception and clinical measures correlated with lesioned hemisphere diffusion parameters. With increasing age, FA increased while MD, RD, AD, and fiber count decreased. The lesioned tracts in children with AIS and PVI followed a similar pattern but fell outside the normal range of DCML tract diffusion parameters of typically developing children. No differences were observed in the diffusion variables in the dominant hemisphere DCML tracts which followed a typical developmental trajectory. Our findings suggest clinical relevance of altered structural connectivity in the lesioned DCML sensory tracts in children with perinatal ischemic stroke.

ACKNOWLEDGMENTS

We would like to acknowledge the efforts and support of J Yajure, M Metzler, and M Piitz.

REFERENCES

van der Aa NE, Northington FJ, Stone BS, Groenendaal F, Benders MJNL, Porro G, Yoshida S, Mori S, de Vries LS, Zhang J (2013): Quantification of white matter injury following neonatal stroke with serial DTI. Pediatr Res 73:756–762.

Andersen RA (1997): Multimodal integration for the representation of space in the posterior parietal cortex. Philos Trans R Soc Lond B Biol Sci 352:1421–1428.

Auld ML, Boyd R, Moseley GL, Ware R, Johnston LM (2012): Tactile function in children with unilateral cerebral palsy compared to typically developing children. Disabil Rehabil 34: 1488–1494.

Avants BB, Epstein CL, Grossman M, Gee JC (2008): Symmetric diffeomorphic image registration with cross-correlation: Evaluating automated labeling of elderly and neurodegenerative brain. Med Image Anal 12:26–41.

Avants BB, Tustison NJ, Song G, Cook PA, Klein A, Gee JC (2011): A reproducible evaluation of ANTs similarity metric performance in brain image registration. NeuroImage 54: 2033–2044.

Basser PJ, Pierpaoli C (1996): Microstructural and physiological features of tissues elucidated by quantitative-diffusion-tensor MRI. J Magn Reson B 111:209–219.

Bax M, Goldstein M, Rosenbaum P, Leviton A, Paneth N, Dan B, Jacobsson B, Damiano D (2005): Proposed definition and classification of cerebral palsy, April 2005. Dev Med Child Neurol 47:571–576.

Bleyenheuft Y, Gordon AM (2013): Precision grip control, sensory impairments and their interactions in children with hemiplegic cerebral palsy: A systematic review. Res Dev Disabil 34: 3014–3028.

Bourke-Taylor H (2003): Melbourne assessment of unilateral upper limb function: Construct validity and correlation with the pediatric evaluation of disability inventory. Dev Med Child Neurol 45:92–96.

de Campos AC, Kukke SN, Hallett M, Alter KE, Damiano DL (2014): Characteristics of bilateral hand function in individuals with unilateral dystonia due to perinatal stroke: Sensory and motor aspects. J Child Neurol 29:623–632.

Chang WH, Kim Y-B, Ohn SH, Park C, Kim ST, Kim Y-H (2009): Double decussated ipsilateral corticospinal tract in schizencephaly. [Miscellaneous Article]. Neuroreport 20:1434–1438.

Coderre AM, Zeid AA, Dukelow SP, Demmer MJ, Moore KD, Demers MJ, Bretzke H, Herter TM, Glasgow JI, Norman KE, Bagg SD, Scott SH (2010): Assessment of upper-limb sensorimotor function of subacute stroke patients using visually guided reaching. Neurorehabil Neural Repair 24:528–541.

Dice L (1945): Measures of the amount of ecologic association between species. Ecology 26:297–302.

Dukelow SP, Herter TM, Moore KD, Demers MJ, Glasgow JI, Bagg SD, Norman KE, Scott SH (2010): Quantitative assessment of limb position sense following stroke. Neurorehabil Neural Repair 24:178–187.

Elangovan N, Herrmann A, Konczak J (2014): Assessing proprioceptive function: Evaluating joint position matching methods against psychophysical thresholds. Phys Ther 94:553–561.

Eliasson AC, Krumlinde-sundholm L, Rosblad B, Beckung E, Arner M, Ohrvall AM, Rosenbaum P (2006): The Manual Ability Classification System (MACS) for children with cerebral palsy: Scale development and evidence of validity and reliability. Dev Med Child Neurol 48:549–554.

Fan Y, Lin K, Liu H, Chen Y, Wu C (2015): Changes in structural integrity are correlated with motor and functional recovery after post-stroke rehabilitation. Restor Neurol Neurosci 33: 835–844.

Findlater SE, Desai JA, Semrau JA, Kenzie JM, Rorden C, Herter TM, Scott SH, Dukelow SP (2016): Central perception of position sense involves a distributed neural network - Evidence from lesion-behavior analyses. Cortex J Devoted Study Nerv Syst Behav 79:42–56.

Garraway WM, Akhtar AJ, Gore SM, Prescott RJ, Smith RG (1976): Observer variation in the clinical assessment of stroke. Age Ageing 5:233–240.

Gauthier LV, Taub E, Perkins C, Ortmann M, Mark VW, Uswatte G (2008): Remodeling the brain: Plastic structural brain changes produced by different motor therapies after stroke. Stroke J Cereb Circ 39:1520–1525.

Habas C, Cabanis EA (2007): Anatomical parcellation of the brainstem and cerebellar white matter: A preliminary probabilistic tractography study at 3 T. Neuroradiology 49:849–863.

Herter TM, Scott SH, Dukelow SP (2014): Systematic changes in position sense accompany normal aging across adulthood. J Neuroeng Rehabil 11:43.

Hirayama K, Fukutake T, Kawamura M (1999): "Thumb localizing test" for detecting a lesion in the posterior column-medial lemniscal system. J Neurol Sci 167:45–49.

Hofer S, Frahm J (2006): Topography of the human corpus callosum revisited–comprehensive fiber tractography using diffusion tensor magnetic resonance imaging. NeuroImage 32: 989–994.

Hoon AH, Lawrie WT, Melhem ER, Reinhardt EM, Van Zijl PCM, Solaiyappan M, Jiang H, Johnston MV, Mori S (2002): Diffusion tensor imaging of periventricular leukomalacia shows affected sensory cortex white matter pathways. Neurology 59:752–756.

Hoon AH, Stashinko EE, Nagae LM, Lin DDM, Keller J, Bastian A, Campbell ML, Levey E, Mori S, Johnston MV (2009): Sensory and motor deficits in children with cerebral palsy born preterm correlate with diffusion tensor imaging abnormalities in thalamocortical pathways. Dev Med Child Neurol 51:697–704.

Jang SH, Kwon YH, Lee MY, Lee DY, Hong JH (2012): Termination differences in the primary sensorimotor cortex between the medial lemniscus and spinothalamic pathways in the human brain. Neurosci Lett 516:50–53.

Jaspers E, Byblow WD, Feys H, Wenderoth N (2015): The corticospinal tract: A biomarker to categorize upper limb functional potential in unilateral cerebral palsy. Front Pediatr 3:112.

Kenzie JM, Girgulis KA, Semrau JA, Findlater SE, Desai JA, Dukelow SP (2015): Lesion sites associated with allocentric and egocentric visuospatial neglect in acute stroke. Brain Connect 5: 413–422.

Kirton A (2013): Modeling developmental plasticity after perinatal stroke: Defining central therapeutic targets in cerebral palsy. Pediatr Neurol 48:81–94.

Kirton A, DeVeber G (2013): Life after perinatal stroke. Stroke J Cereb Circ 44:3265–3271.

Kirton A, deVeber G, Pontigon AM, MacGregor D, Shroff M (2008): Presumed perinatal ischemic stroke: Vascular classification predicts outcomes. Ann Neurol 63:436–443.

Kirton A, Shroff M, Visvanathan T, deVeber G (2007): Quantified corticospinal tract diffusion restriction predicts neonatal stroke outcome. Stroke J Cereb Circ 38:974–980.

Kirton A, Armstrong-Wells J, Chang T, deVeber G, Rivkin MJ, Hernandez M, Carpenter J, Yager JY, Lynch JK, Ferriero DM (2011): Symptomatic neonatal arterial ischemic stroke: The International Pediatric Stroke Study. Pediatrics 128:e1402–e1410.

Kitchen L, Westmacott R, Friefeld S, MacGregor D, Curtis R, Allen A, Yau I, Askalan R, Moharir M, Domi T, deVeber G (2012): The pediatric stroke outcome measure: A validation and reliability study. Stroke 43:1602–1608.

Klein A, Andersson J, Ardekani BA, Ashburner J, Avants B, Chiang M-C, Christensen GE, Collins DL, Gee J, Hellier P,

Song JH, Jenkinson M, Lepage C, Rueckert D, Thompson P, Vercauteren T, Woods RP, Mann JJ, Parsey RV (2009): Evaluation of 14 nonlinear deformation algorithms applied to human brain MRI registration. NeuroImage 46:786–802.

Krumlinde-sundholm L, Eliasson A-C (2003): Development of the assisting hand assessment: A Rasch-built measure intended for children with unilateral upper limb impairments. Scand J Occup Ther 10:16–26.

Krumlinde-sundholm L, Holmefur M, Kottorp A, Eliasson AC (2007): The Assisting Hand Assessment: Current evidence of validity, reliability, and responsiveness to change. Dev Med Child Neurol 49:259–264.

Kuczynski AM, Dukelow SP, Semrau JA, Kirton A (2016): Robotic quantification of position sense in children with perinatal stroke. Neurorehabil Neural Repair 30:762–772.

Lacquaniti F, Guigon E, Bianchi L, Ferraina S, Caminiti R (1995): Representing spatial information for limb movement: Role of area 5 in the monkey. Cereb Cortex N Y N 1991 5:391–409.

Lai C, Zhou H-C, Ma X-H, Zhang H-X (2014): Quantitative evaluation of the axonal degeneration of central motor neurons in chronic cerebral stroke with diffusion tensor imaging. Acta Radiol Stockh Swed 55:114–120. (1987):

Lebel C, Gee M, Camicioli R, Wieler M, Martin W, Beaulieu C (2012): Diffusion tensor imaging of white matter tract evolution over the lifespan. Neuroimage 60:340–352.

Lebel C, Beaulieu C (2011): Longitudinal development of human brain wiring continues from childhood into adulthood. J Neurosci off J Soc Neurosci 31:10937–10947.

Lebel C, Walker L, Leemans A, Phillips L, Beaulieu C (2008): Microstructural maturation of the human brain from childhood to adulthood. NeuroImage 40:1044–1055.

Lennartsson F, Holmström L, Eliasson A-C, Flodmark O, Forssberg H, Tournier J-D, Vollmer B (2015): Advanced fiber tracking in early acquired brain injury causing cerebral palsy. AJNR Am J Neuroradiol 36:181–187.

Lincoln N, Crow JL, Jackson JM (1991): The unreliability of sensory assessment. Clin Rehabil 5:273–282.

Mori S, Zhang J (2006): Principles of diffusion tensor imaging and its applications to basic neuroscience research. Neuron 51: 527–539.

Mori S, Oishi K, Jiang H, Jiang L, Li X, Akhter K, Hua K, Faria AV, Mahmood A, Woods R, Toga AW, Pike GB, Neto PR, Evans A, Zhang J, Huang H, Miller MI, van Zijl P, Mazziotta J (2008): Stereotaxic white matter atlas based on diffusion tensor imaging in an ICBM template. NeuroImage 40:570–582.

Nagae LM, Hoon AH, Stashinko E, Lin D, Zhang W, Levey E, Wakana S, Jiang H, Leite CC, Lucato LT, van Zijl PCM, Johnston MV, Mori S (2007): Diffusion tensor imaging in children with periventricular leukomalacia: Variability of injuries to white matter tracts. AJNR Am J Neuroradiol 28: 1213–1222.

Nevalainen P, Pihko E, Mäenpää H, Valanne L, Nummenmaa L, Lauronen L (2012): Bilateral alterations in somatosensory cortical processing in hemiplegic cerebral palsy. Dev Med Child Neurol 54:361–367.

Oishi K, Faria AV, Van Zijl PCM, Mori S (2011): MRI Atlas of Human White Matter. Philadelphia: Elsevier.

Oldfield RC (1971): The assessment and analysis of handedness: The Edinburgh inventory. Neuropsychologia 9:97–113.

Proske U, Gandevia SC (2012): The proprioceptive senses: Their roles in signaling body shape, body position and movement, and muscle force. Physiol Rev 92:1651–1697.

Raju TN, Nelson KB, Ferriero D, Lynch JK (2007): Ischemic perinatal stroke: Summary of a workshop sponsored by the National Institute of Child Health and Human Development and the National Institute of Neurological Disorders and Stroke. Pediatrics 120:609–616.

Randall M, Johnson LM, Reddihough D (1999): The Melbourne Assessment of Unilateral Upper Limb Function. Melbourne: Royal Children's Hospital, Melbourne.

Rose S, Guzzetta A, Pannek K, Boyd R (2011): MRI structural connectivity, disruption of primary sensorimotor pathways, and hand function in cerebral palsy. Brain Connect 1: 309–316.

Roze E, Harris PA, Ball G, Elorza LZ, Braga RM, Allsop JM, Merchant N, Porter E, Arichi T, Edwards AD, Rutherford MA, Cowan FM, Counsell SJ (2012): Tractography of the corticospinal tracts in infants with focal perinatal injury: Comparison with normal controls and to motor development. Neuroradiology 54:507–516.

Schabrun SM, Hillier S (2009): Evidence for the retraining of sensation after stroke: A systematic review. Clin Rehabil 23: 27–39.

Scott SH (2012): The computational and neural basis of voluntary motor control and planning. Trends Cogn Sci 16:541–549.

Semrau JA, Herter TM, Scott SH, Dukelow SP (2013): Robotic identification of kinesthetic deficits after stroke. Stroke 44: 3414–3421.

Semrau JA, Wang JC, Herter TM, Scott SH, Dukelow SP (2015): Relationship between visuospatial neglect and kinesthetic deficits after stroke. Neurorehabil Neural Repair 29:318–328.

Sherrington C (1907): the proprioceptive system, especially in its reflex aspect. Brain 29:467–482. On

Song SK, Sun SW, Ramsbottom MJ, Chang C, Russell J, Cross AH (2002): Dysmyelination revealed through MRI as increased radial (but unchanged axial) diffusion of water. Neuroimage 17:1429–1436.

Staudt M (2010): Reorganization after pre- and perinatal brain lesions. J Anat 217:469–474.

Staudt M, Braun C, Gerloff C, Erb M, Grodd W, Krageloh-Mann I (2006): Developing somatosensory projections bypass periventricular brain lesions. Neurology 67:522–525.

Tizard JP, Paine RS, Crothers B (1954): Disturbances of sensation in children with hemiplegia. J Am Med Assoc 155:628–632.

Tournier J-D, Calamante F, Connelly A (2012): MRtrix: Diffusion tractography in crossing fiber regions. Int J Imaging Syst Technol 22:53–66.

Tsao H, Pannek K, Boyd RN, Rose SE (2013): Changes in the integrity of thalamocortical connections are associated with sensorimotor deficits in children with congenital hemiplegia. Brain Struct Funct 220:307–318.

Tsao H, Pannek K, Fiori S, Boyd RN, Rose S (2014): Reduced integrity of sensorimotor projections traversing the posterior limb of the internal capsule in children with congenital hemiparesis. Res Dev Disabil 35:250–260.

Tyson SF, Hanley M, Chillala J, Selley AB, Tallis RC (2008): Sensory loss in hospital-admitted people with stroke: Characteristics, associated factors, and relationship with function. Neurorehabil Neural Repair 22:166–172.

Van Heest AE, House J, Putnam M (1993): Sensibility deficiencies in the hands of children with spastic hemiplegia. J Hand Surg Am 18:278–281.

Walther M, Juenger H, Kuhnke N, Wilke M, Brodbeck V, Berweck S, Staudt M, Mall V (2009): Motor cortex plasticity in ischemic

perinatal stroke: A transcranial magnetic stimulation and functional MRI study. Pediatr Neurol 41:171–178.

Wann JP (1991): The integrity of visual-proprioceptive mapping in cerebral palsy. Neuropsychologia 29:1095–1106.

Wen H, Alshikho MJ, Wang Y, Luo X, Zafonte R, Herbert MR, Wang QM (2016): Correlation of Fractional Anisotropy With Motor Recovery in Patients With Stroke After Postacute Rehabilitation. Arch Phys Med Rehabil 97:1487–1495.

Wilke M, Staudt M, Juenger H, Grodd W, Braun C, Krageloh-Mann I (2008): Somatosensory system in two types of motor reorganization in congenital hemiparesis: Topography and function. Hum Brain Mapp 30:776–788.

Yoshida S, Hayakawa K, Yamamoto A, Okano S, Kanda T, Yamori Y, Yoshida N, Hirota H (2010): Quantitative diffusion tensor tractography of the motor and sensory tract in children with cerebral palsy. Dev Med Child Neurol 52:935–940.